ROYAL AIRCRAFT ESTABLISHMENT
BEDFORD.

MINISTRY OF AVIATION

AERONAUTICAL RESEARCH COUNCIL

CURRENT PAPERS

Some Measurements in the Vortex Flow Generated by a Sharp Leading Edge having 65 degrees Sweep.

by

N. C. Lambourne and D. W. Bryer

of the Aerodynamics Division, N.P.L.

Some Measurements in the Vortex Flow Generated by a
Sharp Leading Edge having 65° Sweep
- By -
N. C. Lambourne
and
D. W. Bryer
of the Aerodynamics Division, N.P.L.

14th July, 1959

SUMMARY

The report is concerned with the vortex flow which arises
when separation occurs at a highly swept leading edge. Measurements
were made in the flow over flat plates at 15° incidence each having
a sharp leading edge of 65° sweep. The pressure and velocity
distributions both along the axis of the vortex and for one
cross section of the flow are presented together with a preliminary
discussion of their significance.

1.   Introduction

Current research at N.P.L. into the flow over swept and
delta wings includes an extensive programme of measurements in the
vortex flow due to separation from a sharp leading edge. An
opportunity is now taken to present a connected set of results which
raise new and interesting questions regarding the structure of the
vortex flow.

2.   Measurements

The measurements included in this report relate to
sharp-edged lifting plates having 65° leading-edge sweepback and 15°
incidence. Under these conditions the axis of the vortex above the
plate lies in an approximately straight line from the apex. The main
results were obtained at a speed of 80 ft/sec in a 9 ft × 7 ft wind
tunnel with the half-model shown in Fig. 1. The plate had a
completely flat upper surface and was bevelled on the underside to
provide a sharp leading edge. Planes normal to the leading edge were
chosen at stations A, B, C and D for flow exploration and surface
pressure measurements, but only the results obtained for section B and
in explorations along the axis of the vortex are given in this report.

A 5-tube probe which could be positioned and aligned
remotely provided direct measurements of the total head and flow
direction and derived values of the static pressure and velocity at

numerous/

numerous positions in the vortex field. The outside diameter of the
5-tube probe was 0·10 in., this being small in relation to the
dimensions of the vortex field and thought to be acceptable except when
encountering steep gradients in the flow. Information on the intensity
of the pressure fluctuations in the flow field was obtained by replacing
the 5-tube probe by a plain total-head probe aligned with the flow and
connected by tubing to a microphone. Although the significance of these
particular measurements is not perfectly clear, the root-mean-square
output of the microphone is regarded as a measure of the intensity of
the fluctuations in the total-head pressure.

The pressures at positions along the axis of the vortex were
obtained using small individual pitot and static tubes of diameters
0·024 in. and 0·036 in. respectively. The static tube had a single
hole in its surface and initially the tube was carefully aligned along
the axis of the vortex by trial and error adjustment until rotation of
the tube about its axis had no effect on the measured pressure. The
total head pressure was subsequently measured at the same position.

With the flat delta plate shown in Fig. 2 the velocity of
fluid passing along the axis of the vortex was measured in a water
tunnel. A thin filament of dye solution introduced upstream of the
model was so positioned that it travelled along the axis of the vortex.
Periodic interruption of the dye emission enabled the speed with which
each new front moved along the vortex to be obtained from frame-by-frame
analysis of ciné records. The free stream water speeds ranged from
2 in./sec to 16 in./sec.

In both wind tunnel and water tunnel experiments the
measurements were confined to the region ahead of the position of
vortex bursting, which in both cases was downstream of the trailing edge.

3. Results

The notation and reference axes are shown in Fig. 3. For the
purpose of display, the velocity at each measuring position has been
resolved into two components:

  (i) u, the component parallel to the leading edge,
     and

  (ii) a vector (the resultant of v and w) in the
      measuring plane normal to the leading edge.

In Fig. 3 the mid-point of each arrow corresponds to the position of
the measuring point and the length and direction represent the velocity
vector $(v + w)$ whilst contours of equal values of u are given in
Fig. 4. In both diagrams the velocities are expressed as ratios to
the free stream velocity V_o. It must be mentioned that in deducing
these ratios from the pressure measurements, the density has been taken
to be constant throughout the vortex field. The ratios are thus more
precisely ratios of indicated velocity. Also plotted in Fig. 3 is the
distribution of pressure on the upper surface of the plate determined
from surface pressure holes.

The static pressure coefficient $C_p = (p-p_o)/\frac{1}{2}\rho V_o^2$, the
total head pressure decrement $(H_o-H)/\frac{1}{2}\rho V_o^2$ and the microphone output
are shown respectively in Figs. 5, 6 and 7 by contours which have been
obtained by interpolation from the measured values.

                     The/

The pressures measured with the static and total head tubes at several positions along the axis of the vortex are shown in Fig. 8. The values at station B can be regarded as independent measurements of the maximum values appropriate to the main vortex contours of Figs. 5 and 6. From the measurements with the static and total head tubes at the axis of the vortex, a velocity V_A along the axis has been deduced on the assumption that the change of static pressure across the radius of the static tube can be ignored. The results are plotted as the ratio V_A/V_0 in Fig. 9 together with the direct speed measurements made in the water tunnel.

A thorough assessment of the accuracy of the results would be valuable; unfortunately this is not yet possible owing to a lack of experience of measurements in a strong vortex field. At present it is only possible to make comparisons between the few results which have been obtained by more than one method.

A large discrepancy exists between the pressure measured by holes in the upper surface of the plate and the surface static pressure suggested by the 5-tube probe readings. For instance, the peak value of $-C_p$ is about 2·5 by surface pressure measurements (Fig. 3) but less than 2·0 by extrapolation of the contours of Fig. 5. This suggests that the static pressures obtained with the 5-tube probe are too high. This is borne out by tests which showed that the presence of the probe near the surface raised the local static pressure. Very close to the axis of the vortex, the size and form of the 5-tube probe would make the significance of the readings very doubtful. Nevertheless, although a precise extrapolation to the position of the axis cannot be made owing to the steepness of the gradients, the 5-tube probe results are not inconsistent with those from the static and total head tubes.

The water tunnel measurements of the velocity of fluid along the axis of the vortex were intended to corroborate by a different and more direct method the remarkably high velocities deduced from the axial pressure measurements in the wind tunnel. They do in fact confirm the existence of axial velocities in excess of free stream and, in view of the trend with Reynolds number shown by the water-tunnel results in Fig. 9 and the much higher Reynolds number of the wind-tunnel experiment, they suggest that the velocities derived from the pressure measurements are feasible.

From general considerations, errors due to the finite size of the probe and those from any unsteadiness in the vortex position would be expected to decrease the gradients in the transverse distributions of the measured quantities. In addition it is likely that there is some error when the total-head measurements are made in turbulent flow.

4. Discussion

The results comprise the distribution of quantities both along the axis of the vortex and in a plane normal to the leading edge, which, due to the small angle (less than 8°) between the vortex axis and the leading edge, is close to a transverse section of the vortex.

4.1 Velocity field

The character of the main vortex and the position of its central axis are shown by Figs. 3 and 4. The velocity component u normal to the plane of measurements, which is approximately the axial velocity component along the vortex, is greater than the free-stream speed and increases considerably as the axis is approached. The gradient remains very steep even in the vicinity of the vortex axis. The

values/

values of the transverse vector (v + w) show that the angular velocity
about the vortex axis increases as the axis is approached. On physical
grounds, a core of solid body rotation is to be expected. However,
down to a radius of about 0·25 in., below which the 5-tube probe
measurements are likely to be unreliable, no such core has been detected.

Just above the upper surface and close to the leading edge
there is a region which usually contains weak subsidiary vortices.
In the present measurements the most significant feature of this
region is a flow which is mainly parallel to the leading edge and has
velocities approximating to that of the free stream. It is noticeable
that the shear layer between this region and the flow around the leading
edge does not seem to extend far into the vortex field. The
discontinuity across this shear layer involves a considerable change
in flow direction. For instance, in the accompanying diagram at a
point such as S_1 just inboard of the shear layer the results show
the velocity has magnitude $0·99\,V_0$ with a direction almost normal
to the plane of the diagram, whilst at S_2 just outboard of the layer
the velocity is $1·39\,V_0$ at $36°$ to the plane.
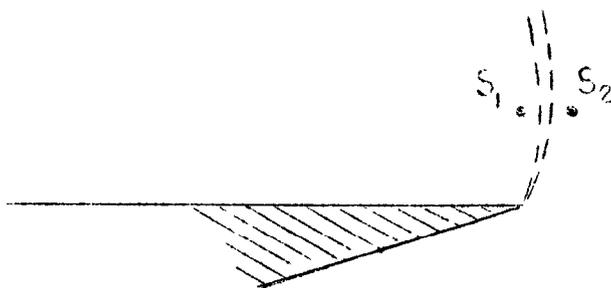
4.2 Pressure field

As shown in Figs. 5 and 6, the static and the total-head
pressures both fall with increasing steepness towards the axis of the
vortex. The low static pressure is associated partly with the
increased velocities in the vortex and partly with the reduction of total
head. Fig. 8 shows that nearly half the reduction in static pressure
at the axis of the vortex is attributable to a reduction of total head.

In view of the very low pressures encountered near the axis of
the vortex it is of some interest to examine the possibility of com-
pressibility effects. It is convenient to consider the ratio of the
static pressure p at a point in the vortex to p_0 the free-stream
static pressure. For a compressible gas we have the relation

$$p/p_0 = 1 + \tfrac{1}{2}\gamma M_0^2\, C_p$$

where M_0 is the free-stream Mach number and C_p is the pressure
coefficient corresponding to pressure p.

At 80 ft/sec ($M_0 \simeq 0·07$), the wind speed of the present tests,
the value of C_p measured at the vortex axis at station B was
approximately -13. Now if the value of the pressure coefficient
remained the same when the speed was increased to correspond to
$M_0 = 0·23$ the value of p/p_0 would be approximately $0·5$ and the
vortex field would be modified by density and temperature changes.
This is confirmed at 180 ft/sec ($M_0 \simeq 0·16$) by a reduced temperature
indicated by a thermocouple placed near the axis of the vortex and,
under suitable conditions of humidity, by the condensation of water
vapour. In practice the value of C_p must increase from -13 with

increasing Mach number, certainly before the value M_o = 0·33 is reached for otherwise the pressure in the vortex would fall to absolute vacuum.

In addition to the minimum at the axis of the vortex, two other regions of reduced total head exist (Fig. 6), one in the region just inboard of the leading edge, the other corresponding to the shear layer from the leading edge and forming a total-head valley which curls into the vortex.

The contours of microphone output (Fig. 7) curl into the vortex in a manner similar to that of total head (Fig. 6). There is a region of maximum intensity of fluctuations at the axis and another at some distance along the shear layer from the leading edge, but in the immediate neighbourhood of the leading edge there is a remarkable absence of fluctuations. It would appear then that the shear layer leaving the leading edge is initially laminar and steady, but becomes turbulent in the region of maximum fluctuation intensity.

The cause of the intense fluctuations at the axis of the vortex is not yet understood but further measurements at other stations should help. At least three possibilities exist:-

(1) The fluctuations generated by the turbulent breakdown of the shear layer are convected into the vortex field. The maximum intensity near the axis is a result of a central "focussing" of the disturbances diffused from the particle paths which are nearly cylindrical spirals.

(2) Fluctuations are generated everywhere in the vortex field particularly near the axis where high shears exist.

(3) The fluctuations originate in the tunnel wall boundary layer some of which enters the vortex at the apex of the model.

With regard to (2) above it can be pointed out that generation of turbulence everywhere along the axis of the vortex would be expected to be accompanied by a reduction of total head with distance along the axis. Fig. 8 shows that except near the apex, the distribution of total head along the axis is almost flat and even shows a slight tendency to rise. However the absence of a falling total-head pressure might be due to the radial inflow of fluid of higher total head rather than to an absence of turbulence generation.

In view of the magnitude of the fluctuations near the axis in relation to that usually encountered in a turbulent boundary layer, the authors believe that possibility (3) above is unlikely.

4.3 Measurements along the axis of the vortex

The mechanism by which the excess velocity along the axis of the vortex is produced and maintained is a matter of considerable interest and speculation. The wind-tunnel results show a favourable pressure gradient and an axial velocity increasing with distance from the apex. There is the possibility that the velocity components parallel to the axis of the vortex are a direct consequence of a pressure distribution prescribed by the rotational velocity components. Then if with increasing distance from the apex these rotational components are augmented in some manner by the vorticity generated by the flow around the leading edge, such a mechanism could explain the falling static pressure along the axis.

Furthermore/

Furthermore the measured increase of axial velocity along the axis must entail a radial inflow component towards the axis of the vortex. On the assumption that angular momentum is conserved, the tightening of the spiral paths tends to increase the rotational components in the region of the axis.

The water-tunnel measurements can be interpreted to suggest a trend with Reynolds number of the velocity along the vortex axis. However, it must be pointed out that there was a noticeable increase in stream turbulence between the flow for $R = 0 \cdot 1 \times 10^5$ and that for $R = 0 \cdot 3 \times 10^5$; this itself may have a significant effect on the axial velocity.

Arising from a consideration of the flow over a delta of infinite extent, it would be expected that for a finite wing, the axial velocity ratio at any position well upstream of the trailing edge could be considered as a function of a local Reynolds number depending on the distance from the apex. An analysis on this basis would be of interest and will be attempted when measurements over a suitable range of conditions have been obtained. Although the water-tunnel measurements already made have been used to obtain the mean fluid velocity over finite lengths of the vortex axis, they are not sufficiently accurate for an analysis involving variations along the axis.

5. Further Work

Similar measurements at other stations along the plate and for other angles of sweepback and incidence are already planned or in progress; these will include an attempt to obtain more detailed information on the flow close to the leading edge. In addition it is intended to investigate Reynolds number effects, also compressibility effects including the temperature field.

Another aspect which is being covered concerns the mechanism of vortex bursting.

6. Acknowledgements

FIG. 1.

Tunnel wall

65°

9·2"

12"

15"

18"

12"

66·20"

A

B

C

D

x

x

26·4"

16°

Section x x
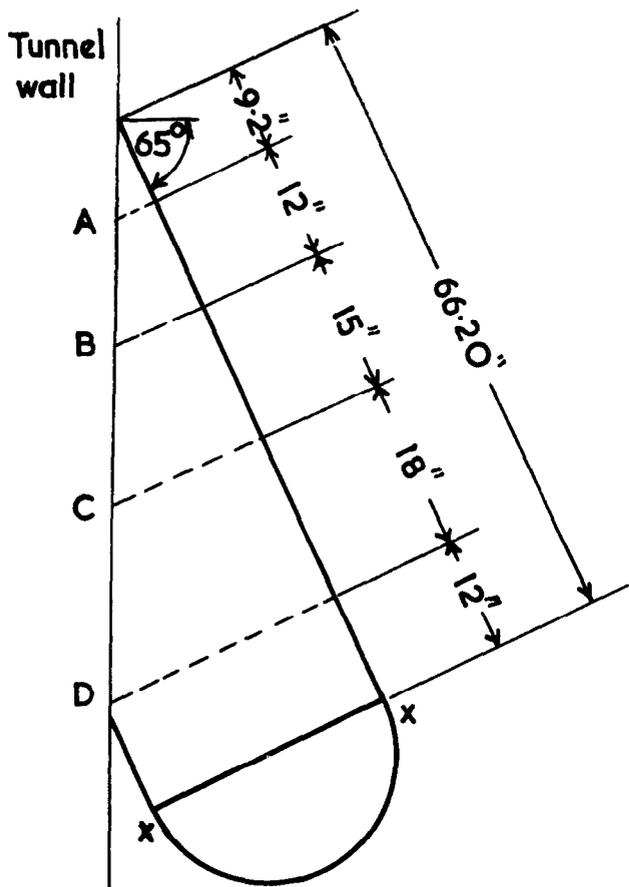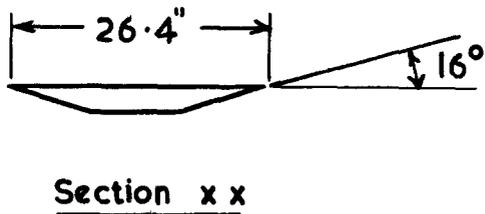
Sharp-edged plate. 9 ft x 7 ft wind tunnel.

FIG. 2.

65°

8·5"

16°

3/16
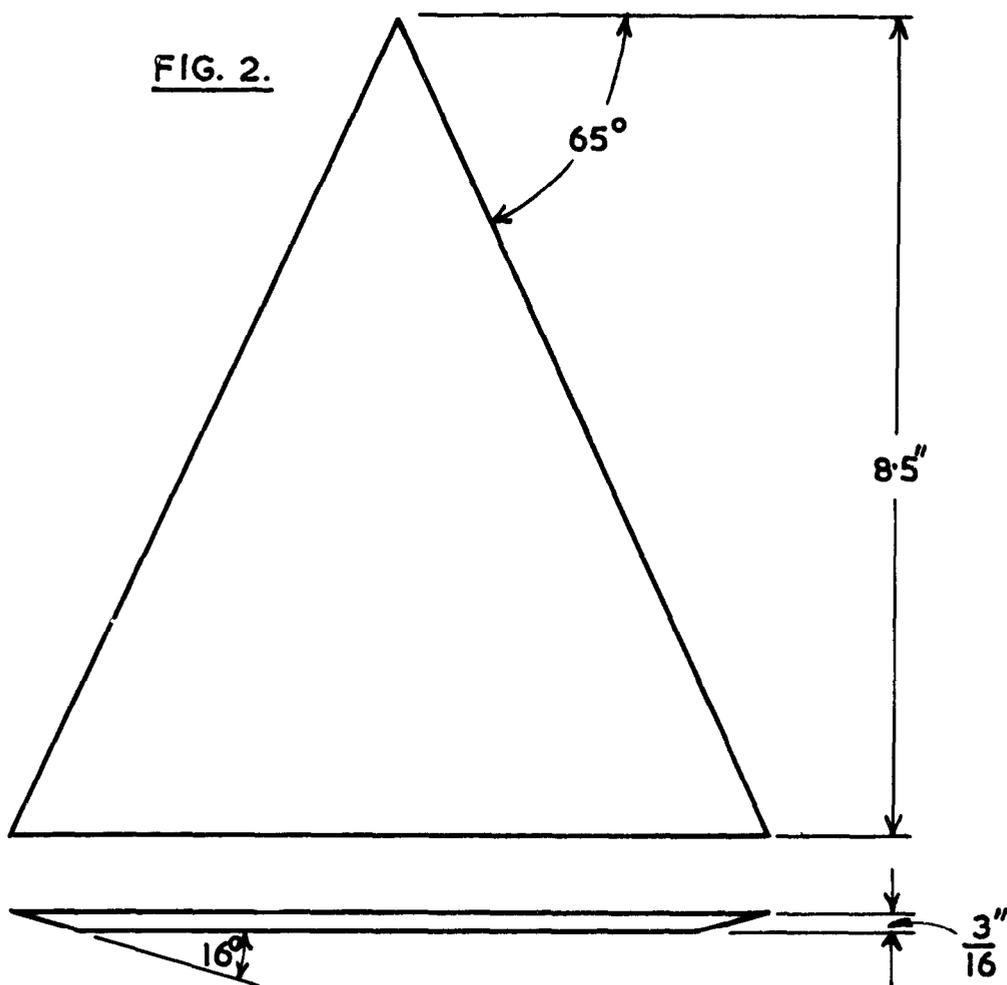
Sharp-edged delta plate. Water tunnel.

FIG. 3.

Reference axes with
origin at leading-edge
of plate.
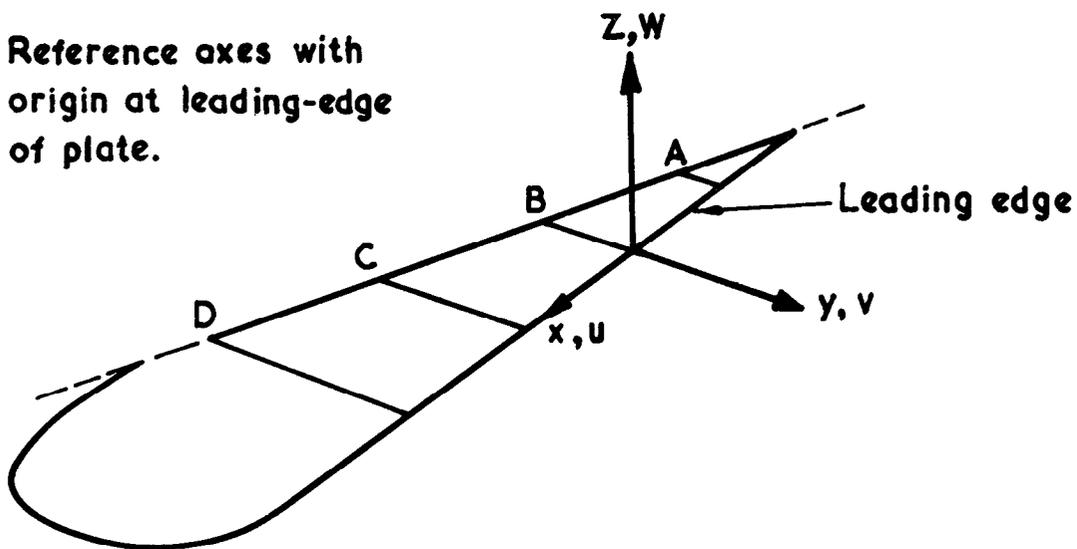
## Transverse velocity vectors $(v+w)/V_o$ in plane normal to leading-edge (Station B)

FIGS. 4. & 5.

FIG. 4.

Velocity component normal to plane of measurement. Contours of u/V
(Station B)

FIG. 5.

Static pressure. Contours of −C_p (Station B)
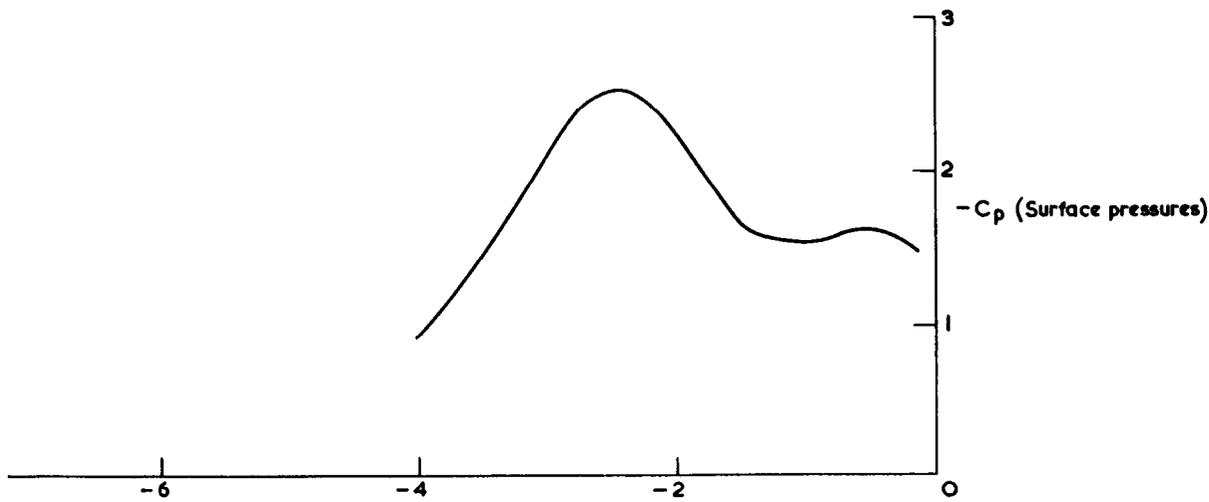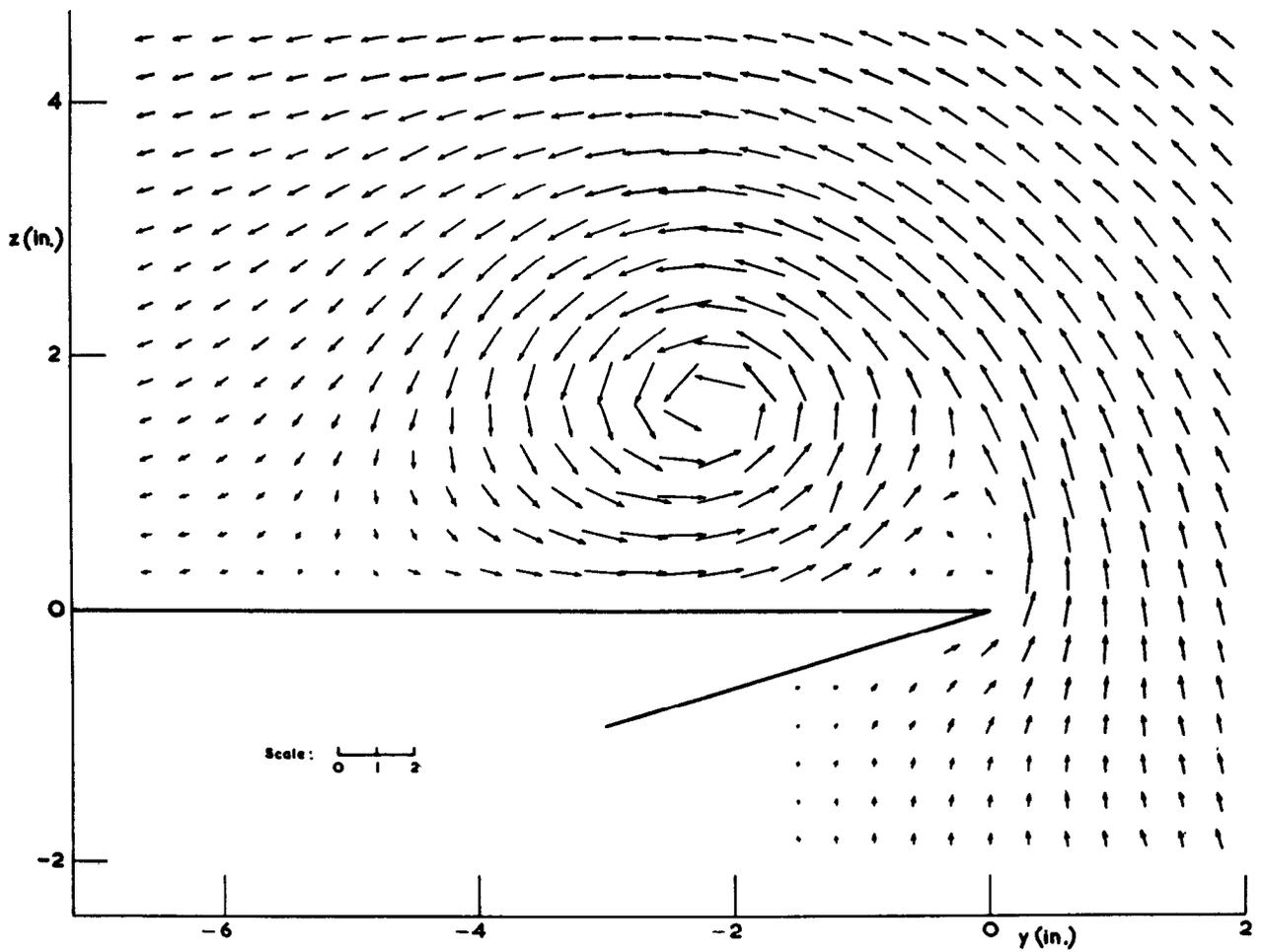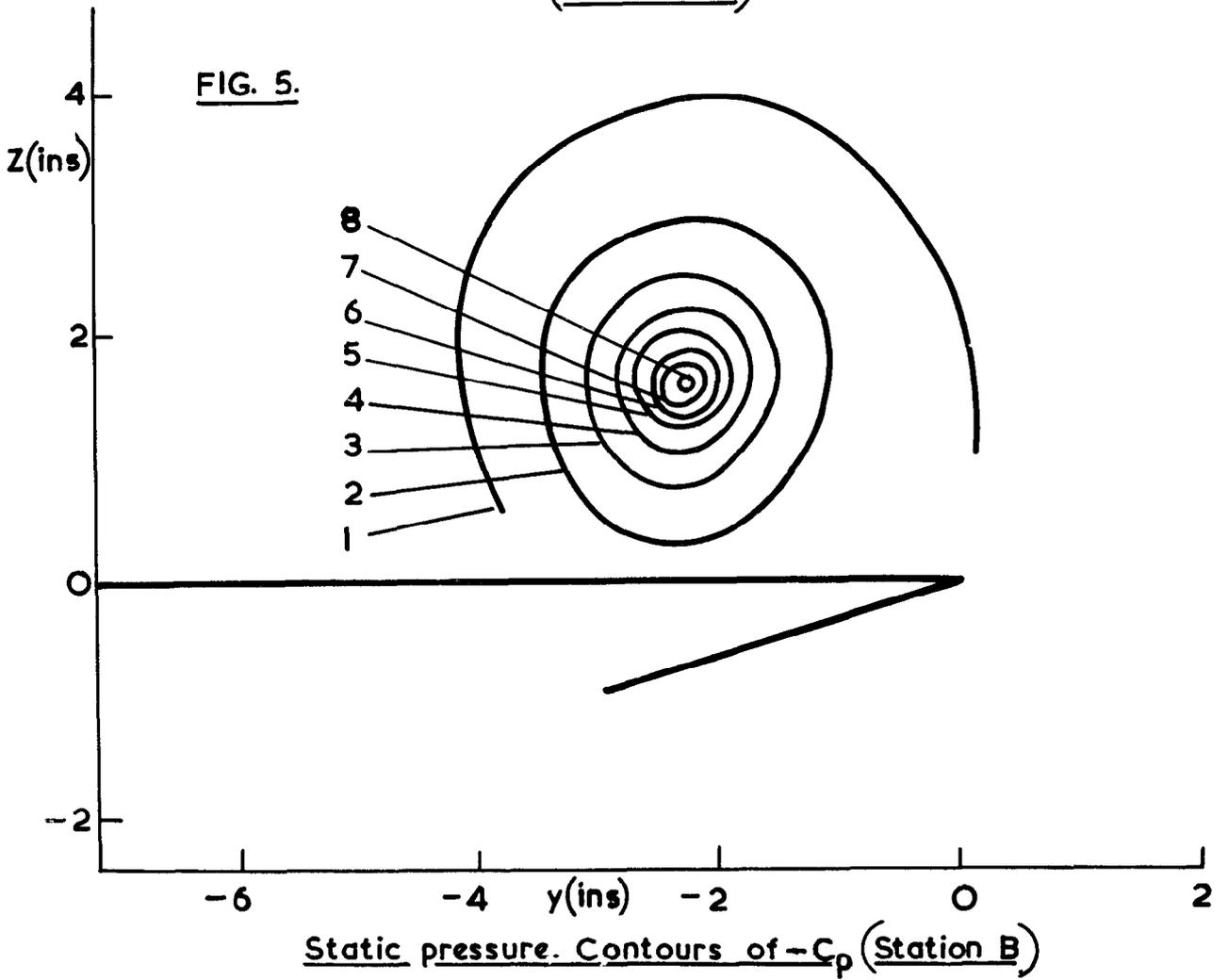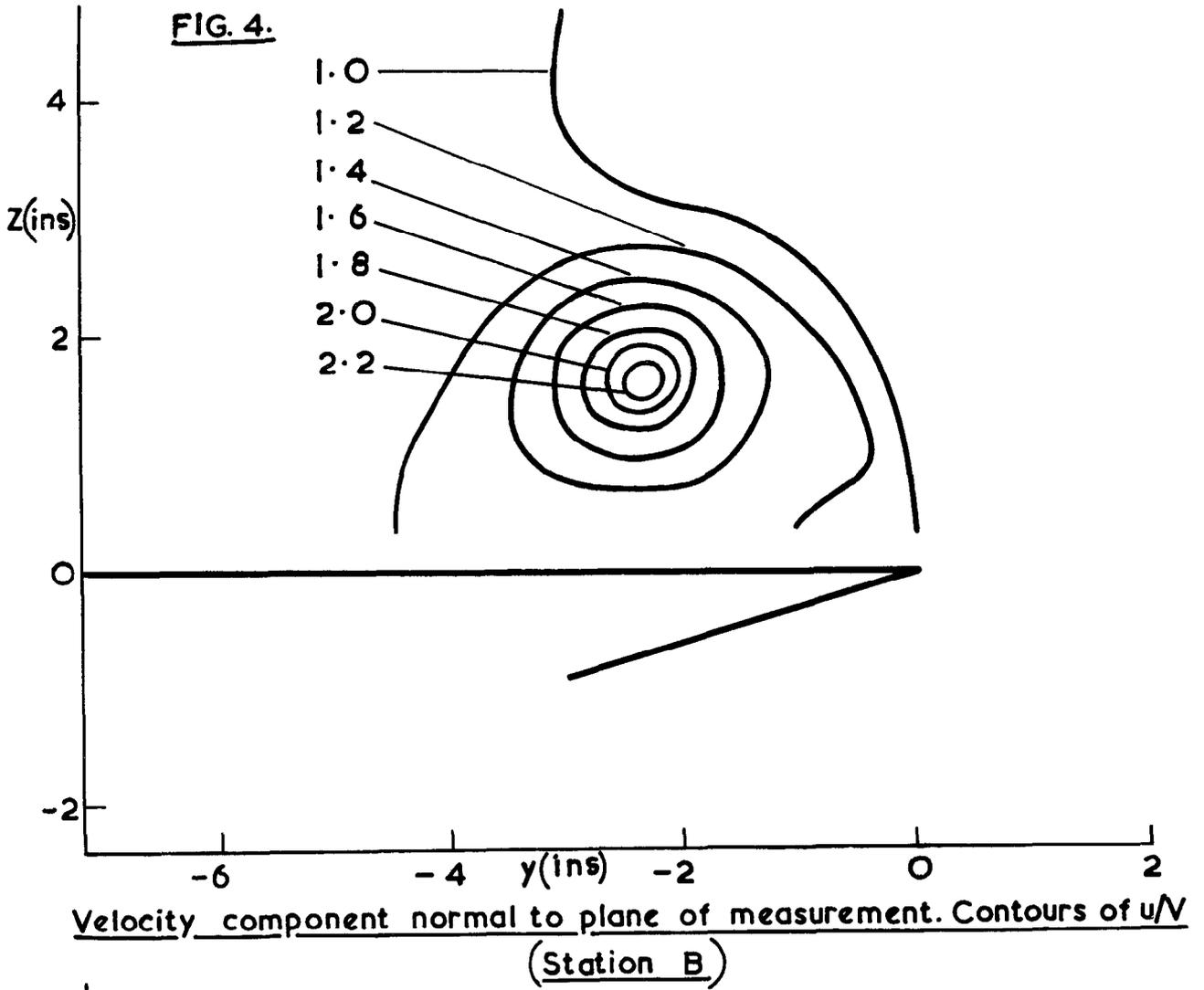
FIGS. 6 & 7.

FIG. 6.
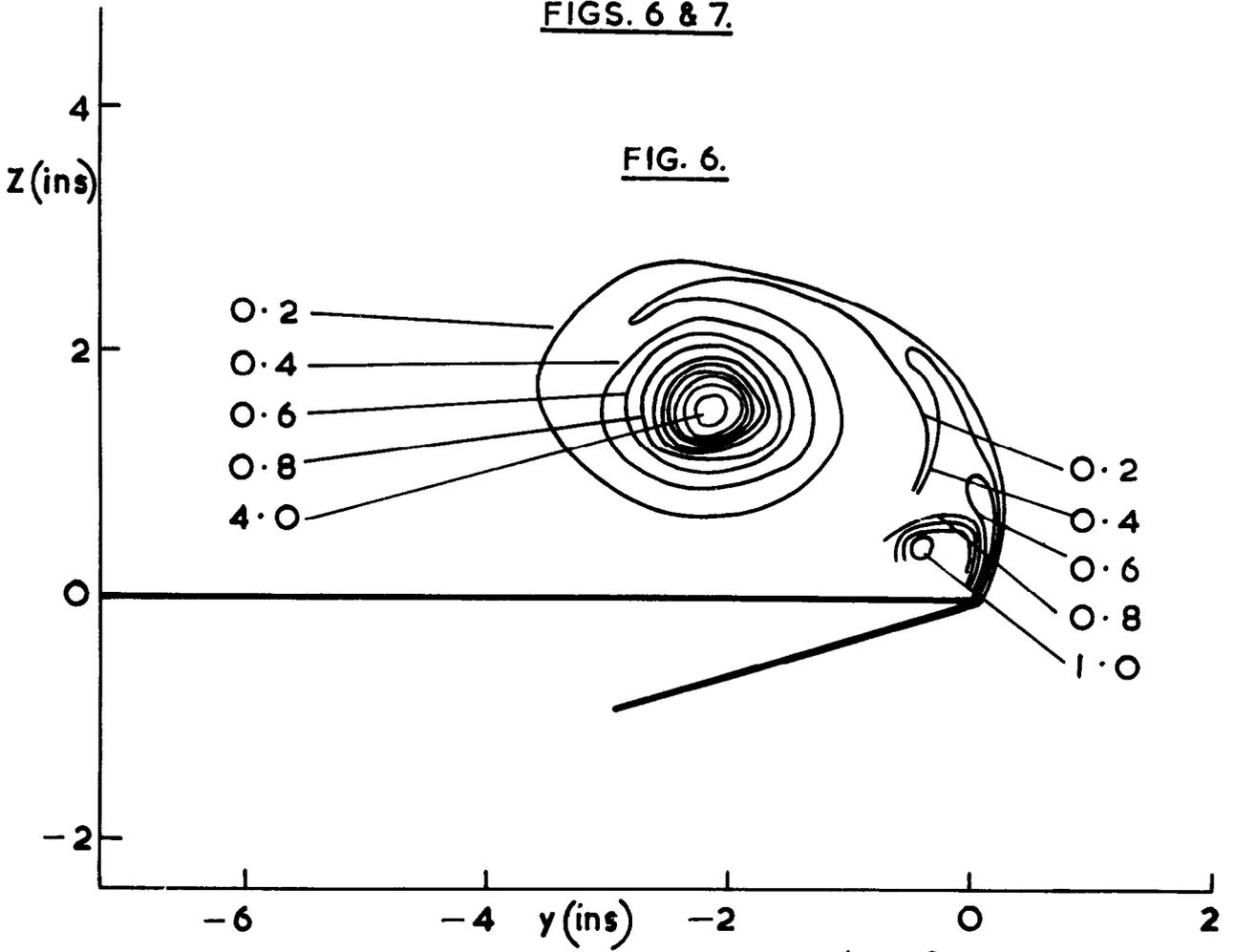
Contours of total-head decrement $\Delta H / \frac{1}{2} \rho V_o^2$ (Station B)

FIG. 7.
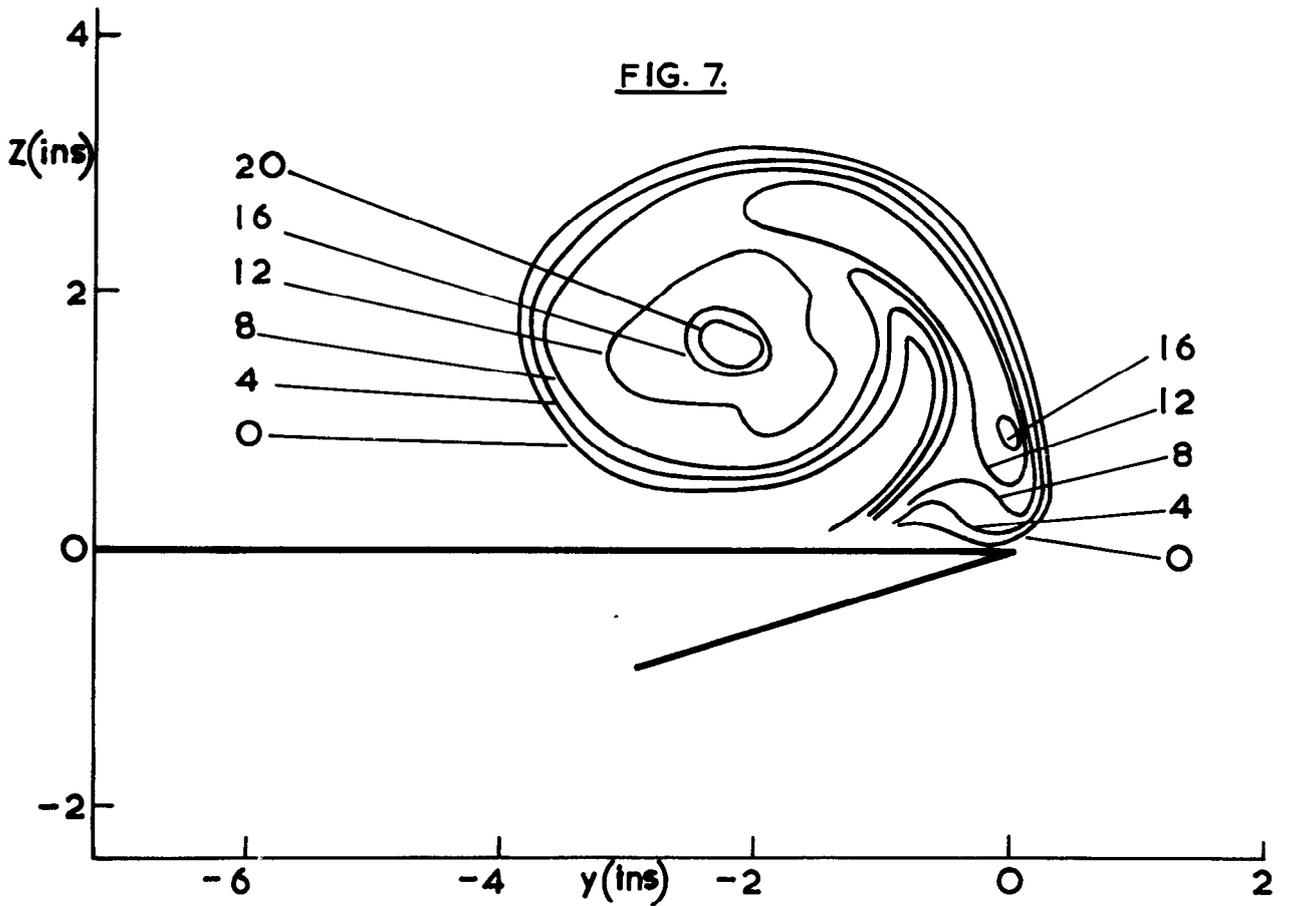
Contours of microphone output (Station B)
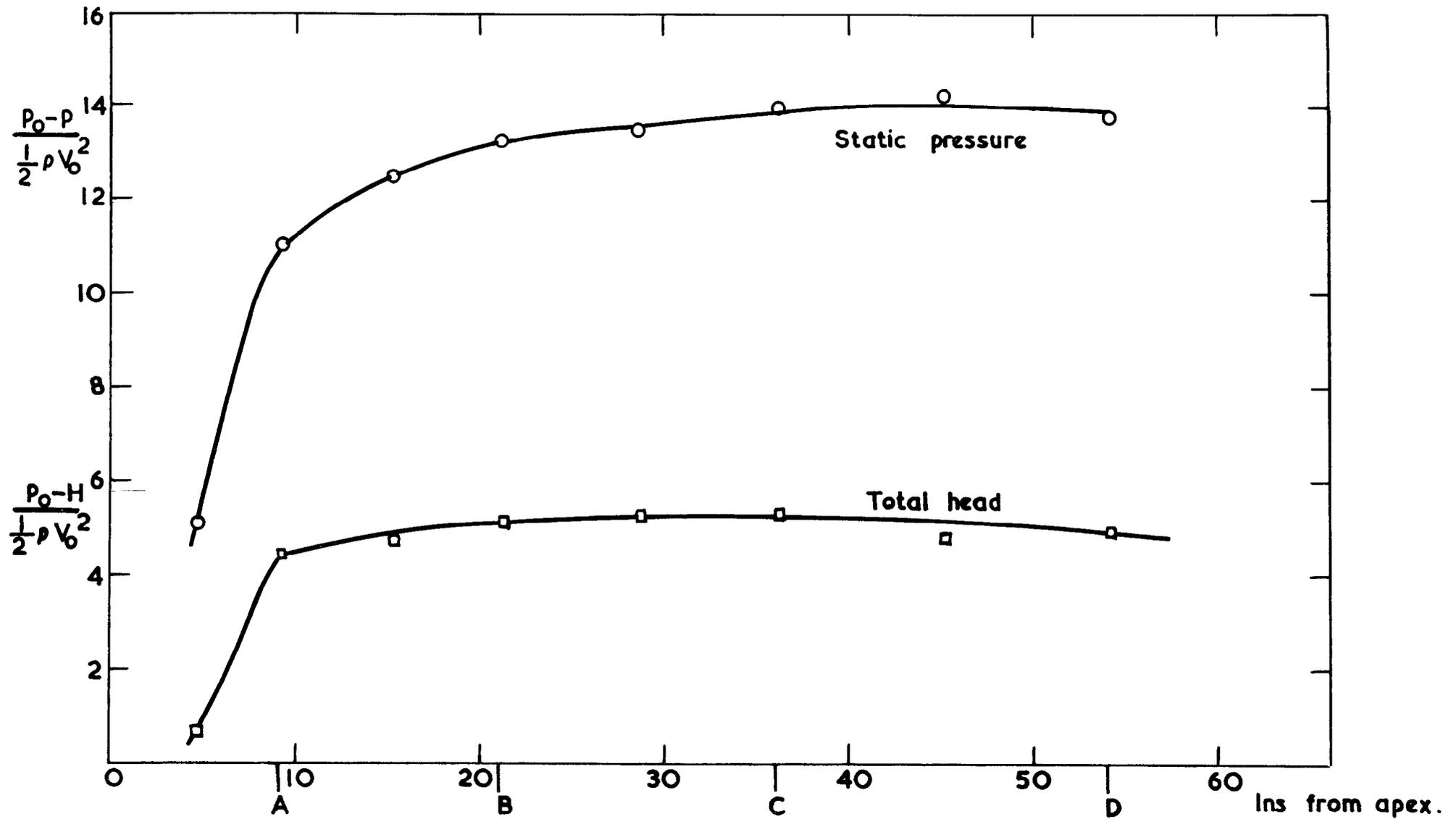
Total head and static pressure measured at axis of vortex. $\Lambda = 65^\circ$, $\epsilon = 15^\circ$ $V_0 = 80$ ft/sec.

FIG.8
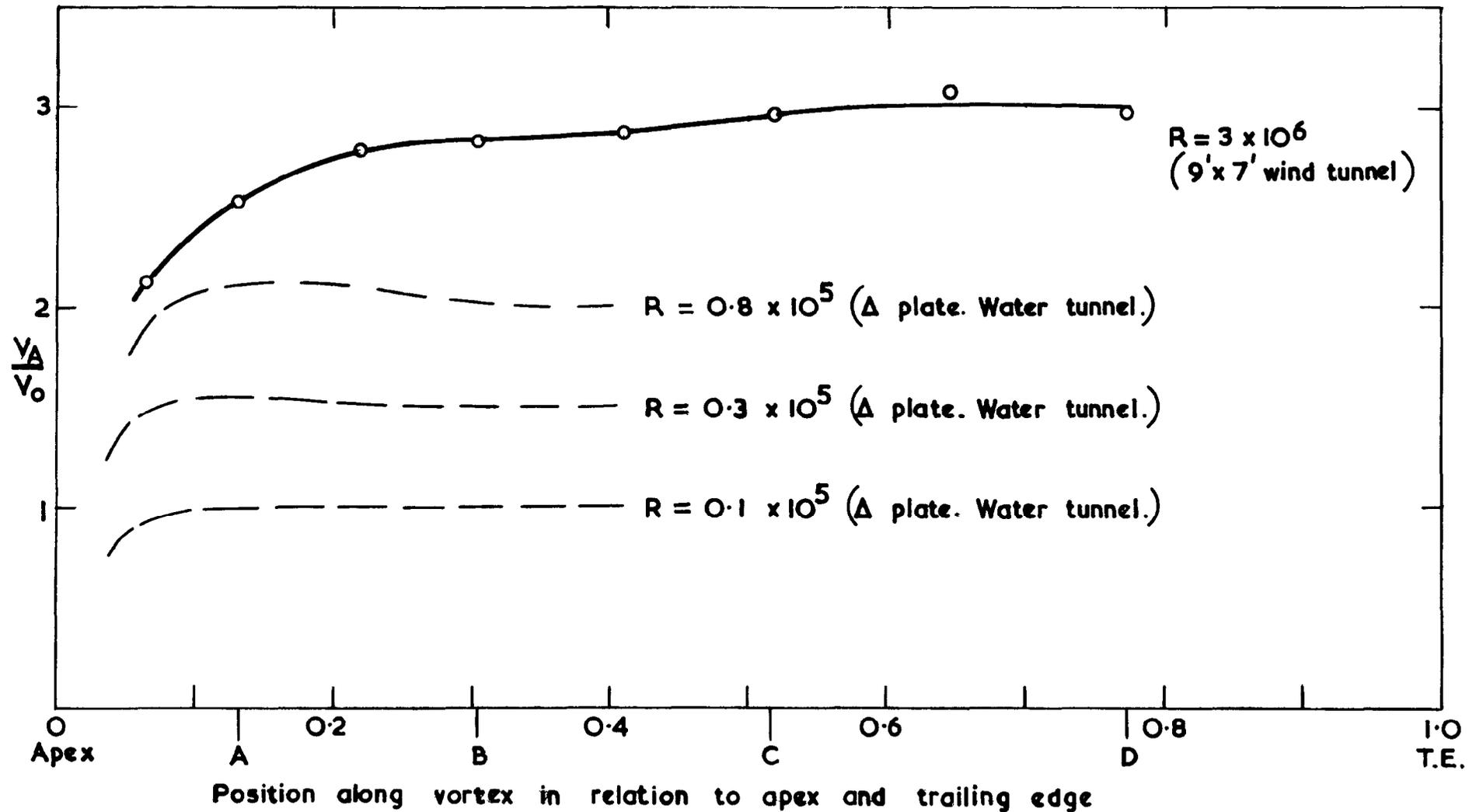
Axial velocities measured at axis of vortex. $\Lambda = 65°$, $\alpha = 15°$

(Reynolds Nos based on distance from apex to trailing edge.)